Chapter-1

Introduction and Literature Review

CHAPTER-1

INTRODUCTION

1.1 Requirement for renewable energy

To fulfill the ever-increasing energy demands to sustain the continuous growth and development of society has increased the inaccessible burden on fossil fuel resources and that is why the struggle to control the energy resources, especially fossil fuels (such as oil, natural gas, and coal), which are limited in supply, is globally visible due to unevenly distribution on earth and the non-renewable nature of generation (millions of years) and the energy supply based on fossil fuels are decisively adding to climate change concerns and global warming [1]. Continuous increasing utilization of fossil fuels to cater to our energy needs also increases net carbon addition and release of toxic exhaust such as SOx, NOx, and unburnt hydrocarbons to the environment and is the root cause of global warming. Further, the depletion of fossil fuel cause worries due to fluctuating high prices for crude oil and coal. Thus both economic and environmental concerns force society to look for alternative renewable energy solutions to cater to the ever-increasing energy needs of the world. Thus renewable energy generation (including solar energy, wind energy, geothermal energy, etc.) has drawn significant attention as an alternative to fossil fuels and a remedy of concern related to pollution, global warming, and climate change due to net carbon addition in earth environment[2].

1.2 Renewable energy sources:

1.2.1 Solar Energy

Solar energy is the most abundant of all energy resources and can even be harnessed in cloudy weather. The rate at which solar energy is intercepted by the Earth is about 10,000

times greater than the rate at which humankind consumes energy. Solar technologies can deliver heat, cooling, natural lighting, electricity, and fuels for a host of applications. Solar technologies convert sunlight into electrical energy either through photovoltaic panels or through mirrors that concentrate solar radiation. Although not all countries are equally endowed with solar energy, a significant contribution to the energy mix from direct solar energy is possible for every country. The cost of manufacturing solar panels has plummeted dramatically in the last decade, making them not only affordable but often the cheapest form of electricity. Solar panels have a lifespan of roughly 30 years, and come in variety of shades depending on the type of material used in manufacturing[3].

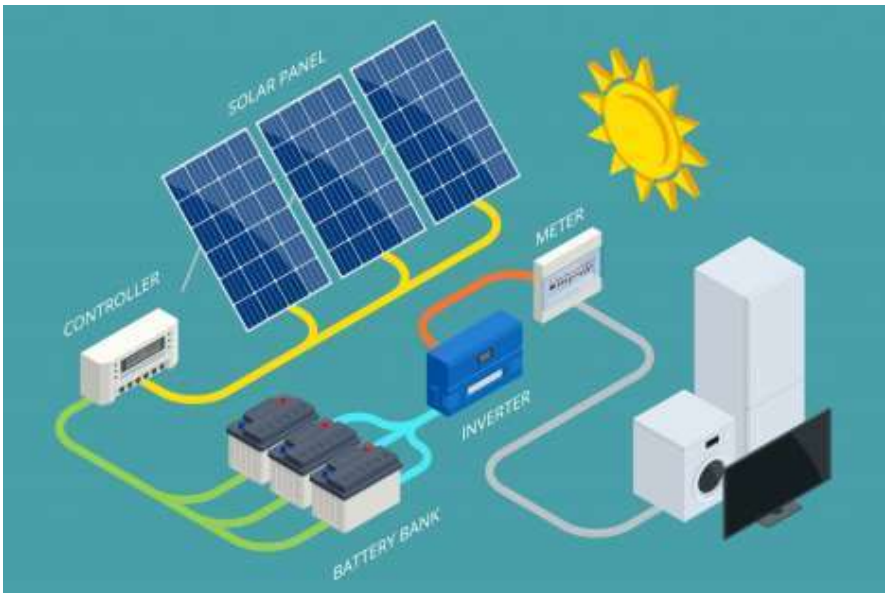

Figure 1.1- Solar energy working[4]. (Figure is taken from open access internet source)

1.2.2 Wind Energy

Wind energy harnesses the kinetic energy of moving air by using large wind turbines located on land (onshore) or in the sea- or freshwater (offshore). Wind energy has been used for millennia, but onshore and offshore wind energy technologies have evolved over the last few years to maximize the electricity produced - with taller turbines and larger rotor diameters.

Though average wind speeds vary considerably by location, the world's technical potential for wind energy exceeds global electricity production, and ample potential exists in most regions of the world to enable significant wind energy deployment. Many parts of the world have strong wind speeds, but the best locations for generating wind power are sometimes remote ones. Offshore wind power offers tremendous potential [3].

Figure:1.2- wind energy[4]. (Figure is taken from open access internet source)

1.2.3 Geothermal energy

Geothermal energy utilizes the accessible thermal energy from the Earth's interior. Heat is extracted from geothermal reservoirs using wells or other means. Reservoirs that are naturally sufficiently hot and permeable are called hydrothermal reservoirs, whereas reservoirs that are sufficiently hot but that are improved with hydraulic stimulation are called enhanced geothermal systems. Once at the surface, fluids of various temperatures can be used to generate electricity. The technology for electricity generation from hydrothermal reservoirs is mature and reliable and has been operating for more than 100 years[3].

Figure: 1.3- Geothermal energy[6] (Figure is taken from open access internet source)

1.2.4 Hydropower

Hydropower harnesses the energy of water moving from higher to lower elevations. It can be generated from reservoirs and rivers. Reservoir hydropower plants rely on stored water in a reservoir, while run-of-river hydropower plants harness energy from the available flow of the river. Hydropower reservoirs often have multiple uses - providing drinking water, water for irrigation, flood and drought control, navigation services, as well as energy supply. Hydropower currently is the largest source of renewable energy in the electricity sector. It relies on generally stable rainfall patterns and can be negatively impacted by climate-induced droughts or changes to ecosystems that impact rainfall patterns. The infrastructure needed to create hydropower can also impact ecosystems in adverse ways. For this reason, many consider small-scale hydro a more environmentally-friendly option, and especially suitable for communities in remote locations[3].

Figure 1.4: Hydrothermal energy[7] (Figure is taken from open access internet source)

1.2.5 Ocean energy

Ocean energy derives from technologies that use the kinetic and thermal energy of seawater waves or currents for instance - to produce electricity or heat. Ocean energy systems are still at an early stage of development, with several prototype wave and tidal current devices being explored. The theoretical potential for ocean energy easily exceeds present human energy requirements[3].

Figure 1.5: Ocean energy[8] (Figure is taken from open access internet source)

1.2.6 Bioenergy

Bioenergy is produced from a variety of organic materials, called biomass, such as wood, charcoal, dung, and other manures for heat and power production, and crops for liquid biofuels. Most biomass is used in rural areas for cooking, lighting, and space heating, generally by poorer populations in developing countries. Modern biomass systems include dedicated crops or trees, residues from agriculture and forestry, and various organic waste streams. The energy created by burning biomass creates greenhouse gas emissions, but at lower levels than burning fossil fuels like coal, oil, or gas. However, bioenergy should only be used in limited applications, given potential negative environmental impacts related to large-scale increases in forest and bioenergy plantations, and resulting deforestation and land-use change[3].

Figure 1.6: Bioenergy[9] (Figure is taken from open access internet source)

1.2.7 Challenges with the renewable energy sources

The qualities of renewable energies are often overshadowed by one of their defaults: they produce intermittently and more or less predictably. In other words, it is difficult to rely on them systematically to integrate their production in a general and global pattern of power

supply [10]. The electricity generated through the renewables can not be connected to the grid directly due to the very high power and current fluctuation attached to these renewable sources as solar intensities or wind speed can not be controlled or programmed; they are weather and time-dependent. To ensure a balance between supply and demand at all times and everywhere, it seems essential to develop solutions to store the energy generated through renewable sources [11].

1.3 Renewable Energy Storage Solutions:

Several energy storage solutions are available and are in practice. Their advantages and their shortcoming are listed below:

1.3.1 Mechanical energy storage

The flywheel energy storage system (FESS) is a mechanical storage device that emulates the storage of electrical energy by converting it to kinetic energy which is stored in a rotating mass with very low frictional losses [12]. The input energy to the FESS is usually drawn from an electrical source coming from the grid or any other source of electrical energy. An integrated motor-generator speeds up as it stores energy and slows down when it is discharging.

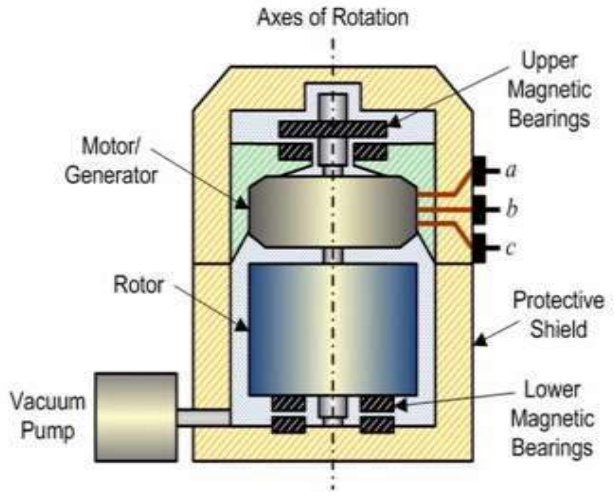

Figure 1.7: Structure and components of a flywheel [13]. (Figure is taken from open access internet source)

1.3.2 Hydrogen Energy Storage and Methanation

Water electrolysis technology is the most flexible and tenable solution to store renewable energy on a large, long-term scale. Using excess renewable electricity the Proton Exchange Membrane (PEM) splits water into its constituent parts, hydrogen, and oxygen, that can be stored in common tanks.[14,15]

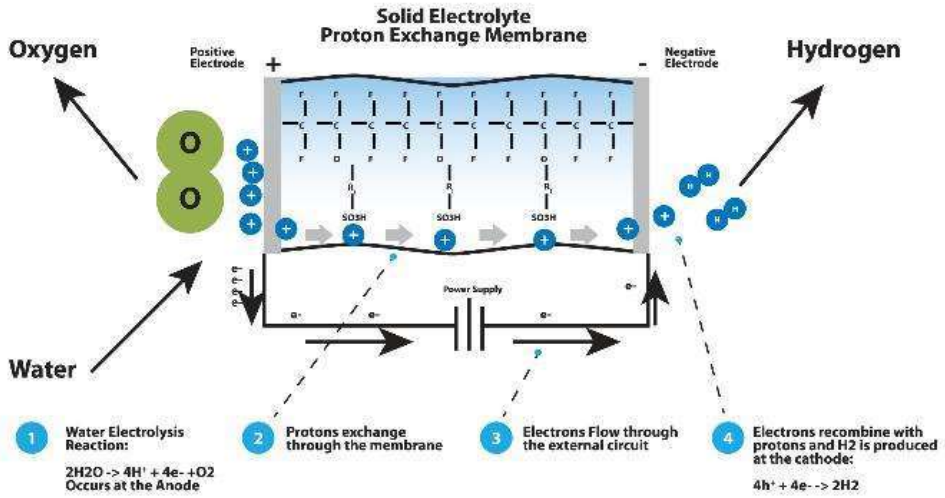

Figure 1.8: Scheme of the chemical process of hydrogen production [16]. (Figure is taken from open access internet source)

1.3.3 Superconducting Magnetic Energy Storage (SMES)

The system consists of three major components: the coil, the power conditioning system (PCS), and a cooling system. The idea is based on the fact that a current will continue to flow in a superconductor even after the voltage across it has been removed. When the superconductor coil is cooled below its superconducting critical temperature it has negligible resistance, hence current will continue to flow (even after a voltage source is disconnected) [17, 18]. The energy is stored in the form of a magnetic field generated by the current in the superconducting coil. It can be released by discharging the coil.

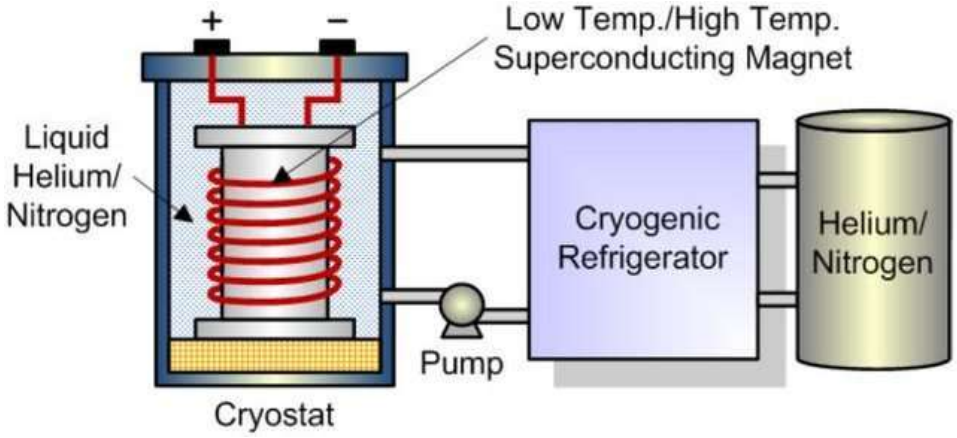

Figure 1.9: Scheme of the main component of SMES system [19]. (Figure is taken from open access internet source)

1.3.4 Thermal energy storage

Thermal energy storage (TES) includes several different technologies. Thermal energy can be stored as sensible heat, latent heat, and chemical energy (thermochemical energy storage) using chemical reactions [20]. Thermal energy storage in the form of sensible heat is based on the specific heat of a storage medium, which is usually kept in storage tanks with high thermal insulation[21].

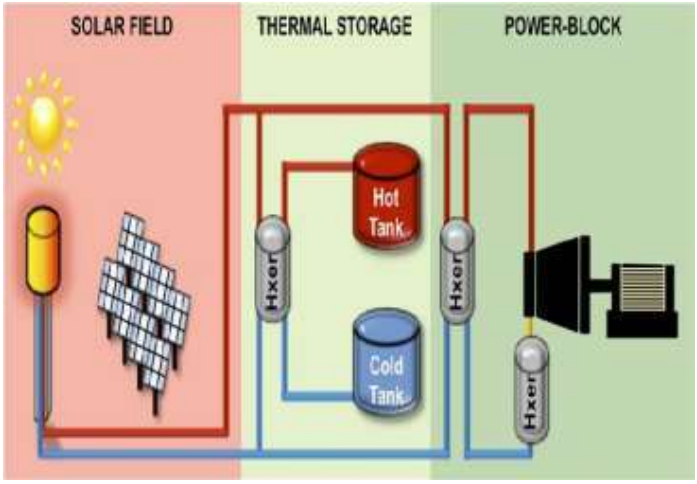

Figure 1.10: scheme of the sensible heat storage installation[22] (Figure is taken from open access internet source)

1.3.5 Electrochemical energy storage devices

Electrochemical energy devices are gaining attention due to their higher conversion efficiency and fast power delivery capabilities. The energy or electricity generated through renewable sources can be stored in the form of chemical energy and the stored chemical energy can be dissipated into electrical energy more efficiently. Thus the electrochemical energy storage devices are also gaining much attention due to their recent achievement in delivering efficient power supply to portable electronics[23,24]. That is why now they are envisaged as energy storage and power delivery solutions for electric vehicles (EVs) and bulk grid-scale energy storage and power delivery solutions for grid regulation through renewable energy sources. Redox flow batteries, metal-air batteries, and pseudocapacitive electrodes enabled Hybrid supercapacitors' are the technology of the future for fulfilling bulk energy storage and fast power delivery requirements.

1.3.6 Historical Perspective

The study of electrochemistry, and the dawn of electricity, began in the late 18th century when Luigi Galvani noted that a frog's leg twitched when touched with a charged metal scalpel. This discovery led Alessandro Volta to develop the first battery, called the Volta pile (Figure 1.11), which consisted of alternating disks of copper and zinc separated by salt water-soaked cardboard or felt. The Volta pile led to the discovery of the electrolysis of water (1800, Nicholson & Carlisle) and the discoveries, within several years (1807-1808), of sodium, potassium, calcium, boron, barium, strontium, and magnesium by Humphry Davy. Michael Faraday used the Volta pile to develop his 1st and 2nd laws of electrochemistry.[25]

Figure 1.11: voltaic pile[26] (Figure is taken from open access internet source)

It is interesting to note that most of the battery technologies in use or development today were invented in the previous two centuries, the exception being the lithium-ion battery (Table 1.1).

Inventor	**Technology**	**Year**
A. Volta	First battery	1800
A. Smee	Metal air batteries	1840
G. Plante	Lead-acid battery	1859
G. Leclanché	Zn-MnO_2 primary battery	1868
T. deMichalowski	Ni-Zn battery	1899
W. Jungner	Ni-Cd battery	1901
Multiple inventors	Li-ion battery	1991

Table 1.1. Development of various battery technologies.[27]

The development of electrochemical capacitors came much later than batteries- more than a century. The first electrochemical capacitor was developed in 1957 when a patent was granted to General Electric for electrical energy storage through the electric double layer at a

porous carbon electrode.[28] Pseudocapacitance was first described in 1971 for RuO_2 by Trasatti and Buzzanca while the theoretical understanding was further developed by Conway[29].

1.3.7 Energetic of the Batteries

EES involves the storage of charge, either directly through electrostatic interactions or indirectly through chemical bonds, on two electrode surfaces separated by an electrolyte. Batteries store electrical energy faradaically, or through the formation of chemical bonds through oxidation/reduction reactions that involve electron transfer. In this device the total energy stored (G) is an integral function of the overall capacity (Q) and voltage (E):

$$G = \int QDE \qquad (1.1)$$

The relationship between capacity and voltage is fundamentally different for batteries. This is because the faradaic reactions utilized in batteries often result in a phase transformation when an electrode material transforms from the oxidized to the reduced form:

$$Q + ne^- \leftrightarrow R \qquad (1.2)$$

For an ideal battery with an invariant potential, the total stored energy is simply:

$$G = QE \qquad (1.3)$$

The theoretical (or maximum) capacity of a battery material can be determined by knowing the redox reaction taking place and by using Faraday's laws of electrolysis which state that:

$$Q = \frac{Fn}{M} \qquad (1.4)$$

where F is the Faraday constant (96,485 C mol^{-1}), n is the number of electrons transferred, and M is the molar mass of the material. The potential of a battery material is directly related to the Gibbs energy change (ΔG) of the redox reaction and thus the chemical potential change (Δμ) upon reduction:[29]

$$E^0 = -\Delta G / nF = -\Delta\mu / nF \qquad (1.5)$$

This relationship forms the basis of the Nernst equation, which also accounts for the different activities of the materials involved in the redox reaction.

1.4 Type of rechargeable energy storage and power delivery technologies:

At present batteries are produced in many sizes for a wide spectrum of applications. Supplied powers move from W to the hundreds of kW (compare battery for power supply of pacemakers and battery for the heavy motor vehicle or power station). Common commercially accessible secondary batteries according to used electrochemical systems can be divided into two basic groups: Standard batteries (lead-acid) and modern batteries (Li-ion).

1.4.1 Lead-acid battery

The lead-acid battery when compared to other electrochemical sources has many advantages. It is low price and availability of lead, good reliability, high voltage of the cell (2 V), high electrochemical effectivity, and cycle life from several hundred to thousands of cycles, lead-acid batteries are suitable for medium and large energy storage applications because they offer a good combination of power parameters and a low price. It is usually composed of some series-connected cells. The main parts of a lead-acid battery are electrodes, separators, electrolytes, vessels with lids, ventilation, and some other elements.[30]

In a lead-acid battery active material is made from lead oxide PbO pasted onto a grid and then electrochemically converted into reddish-brown lead dioxide PbO_2 on the positive electrode and grey spongy lead Pb on the negative electrode, Separators electrically separate the positive electrode from negative and, an aqueous solution of H_2SO_4 is used as electrolyte with the density of 1.22-1.28 g/cm^3.[31]

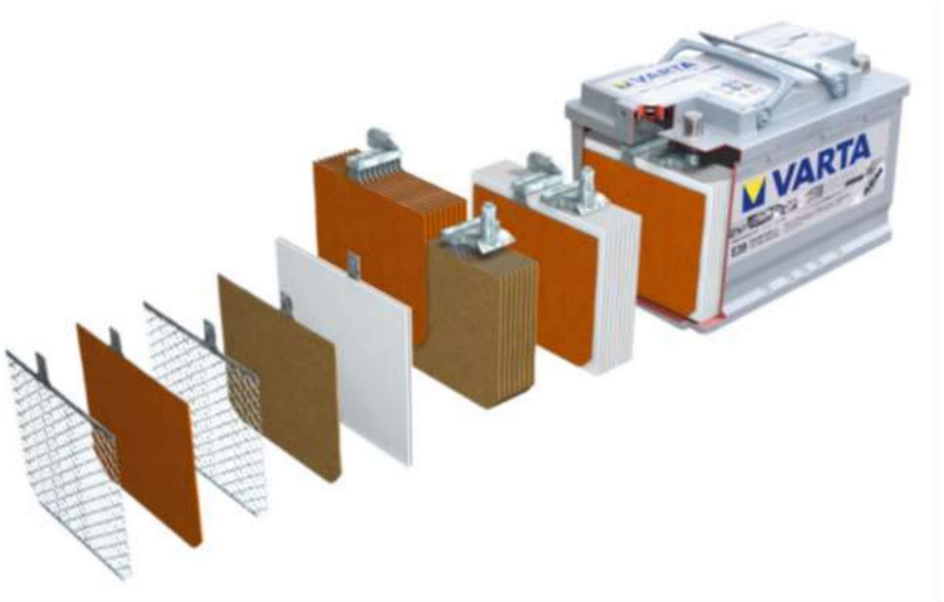

Figure 1.12: Lead-acid battery (Figure is taken from open access internet source)

Overall chemical reaction during discharge is:

$$PbO_2 + Pb + 2H_2SO_4 \rightarrow 2PbSO_4 + 2H_2O \qquad E0 = +2.048\ V \qquad (1.6)$$

The reaction proceeds in opposite direction during charge.

The lead-acid battery is used for cranking automobile internal combustion engines and also for supporting devices that require electrical energy when the engine is not running and the power supply of industrial trucks, delivery vehicles, and stationary battery ensures uninterrupted electric power supply in case of failure in distributing network. The cycle life of the battery is about 5 years (1000 charge-discharge cycles).

Lead-acid batteries can be affected by positive plate expansion, water loss brought about by gassing or by a high temperature, acid stratification, positive grid corrosion, and incomplete charging causing active mass sulphation, due to this battery in a partial state of charge cycling in hybrid electric vehicles (HEV) and for remote area power supply applications)[32].

1.4.2 Lithium-ion battery

Lithium-ion batteries enabled the portable electronics revolution to take place over the past 30 years. Today the batteries utilize reversible lithium-ion intercalation into both the cathode and anode to store energy. While electrochemical insertion of lithium into transition metal compounds was reported in the 1970s,[33] it wasn't until the discovery of lithiated transition metal oxides and lithium intercalation into graphite that the first battery was commercialized by Sony. The basic configuration of a lithium-ion battery is shown in Figure 1.13. The cathode material is usually $LiCoO_2$ while the anode is graphite. The advantage of utilizing these two electrode materials is that they result in a high cell voltage of 3.6 V and an energy density of approximately 120-150 Wh kg^{-1}. [34] The electrolyte is $LiPF_6$ in a mixture of organic solvents such as ethylene carbonate and dimethyl carbonate. The reactions during the energy-storage (charging) stage are:

$$\text{Cathode: } LiCoO_2 \leftrightarrow Li_{1-x}CoO_2 + xLi^+ + xe^- \qquad (1.7)$$

$$\text{Anode: } C_6 + Li^+ + e^- \leftrightarrow LiC_6 \qquad (1.8)$$

These reactions are reversed during the discharge cycle; commercial lithium-ion batteries are rated for approximately 500 charge/discharge cycles.[35]

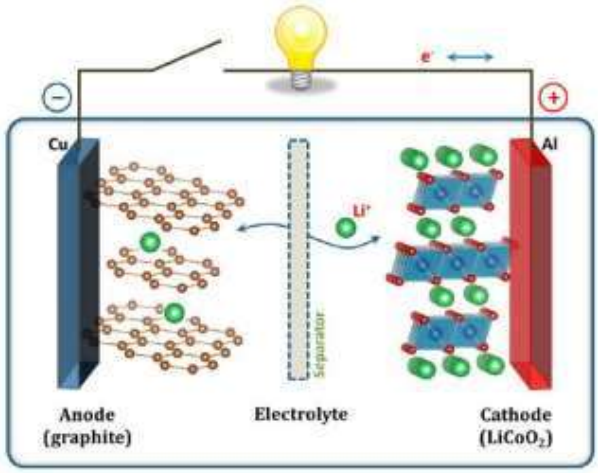

Figure1.13. The configuration of a Li-ion battery is used today[33]. (Figure is taken from open access internet source)

Intercalation reactions can offer a high degree of reversibility due to the small voltage

differences during insertion and de-insertion for many materials. However, outside of their stability limits, intercalation materials experience severe structural changes and dissolution that lead to severe problems such as capacity fading and thermal runaway. Intercalation reactions usually store 1 lithium per formula unit and this value has not increased over the years despite extensive research on the topic. Energy density can also be improved by increasing the voltage of the cathode material from the 3.6-3.9 V of $LiCoO_2$; the voltage of the graphite is already quite low. Several higher voltage cathodes have been proposed, among them a family of materials based on the spinel $Li_yM_xMn_{2-x}O_4$, where M = Cr, Fe, Co, Ni, and Cu.[38] In these materials, the energy storage occurs between 4 and 5 V. The higher voltage route has an additional challenge of finding suitable electrolytes for a 5 V potential window.

1.4.3 Challenges and shortcomings of Li-ion batteries

Despite their technological promise, Li-ion batteries still have several shortcomings, particularly in safety. Li-ion batteries tend to overheat and can be damaged at high voltages. In some cases, this can lead to thermal runaway and combustion[36]. Li-ion batteries are also subject to aging, meaning that they can lose capacity and frequently fail after several years. Another factor limiting their widespread adoption is their cost, which is around 40% higher nevertheless, they are not ideally suited for applications that require fast charge storage, such as regenerative braking[37].

Although significant advancements have been made during the past decades to improve battery performance, the main problem comes from peak usage. Even in small electronic devices such as mobile phones and laptops, battery damage occurs upon sudden usage of the battery's energy. This situation is constant in EVs, as different factors such as driving style, road, etc., cause rapid changes in power consumption. A battery performs well when it is discharged monotonically because the corresponding electrochemical reaction can proceed

monotonically[38]. However, when an EV requires sudden power consumption during its acceleration, the battery pack cannot be discharged quickly enough to satisfy this requirement. The same applies to high current storage in the batteries that are generated during the braking of the EV. These fluctuating flows of a high electric current into and from the battery could have a detrimental effect on the electrolytes. When this acceleration/braking is repetitive (city driving, for example), this can shorten the life of the batteries. hence, there is a need for an alternative to deal with the problem of batteries like their low life span and less power; in the present situation, needs a device that has special abilities such as high power, energy density along with long cycle life[39]. Modern high-power equipment demands a large amount of energy along with quick delivery; batteries and capacitors are unable to provide such requirements[40]. Supercapacitors have been developed in the last few decades to fulfill major requirements of conventional energy storage devices (batteries and capacitors).

1.4.4 Electrochemical Supercapacitors

Electrochemical supercapacitors (ESs) are emerging energy storage devices that offer a balance of power and energy performance and bridge the gap between conventional capacitors and batteries. ESs also possess other advantages such as long cyclic life and the ability to charge-discharge rapidly, making them suitable for applications neither capacitors nor batteries can achieve. Currently, ESs are used for electric vehicles in conjunction with batteries, which have been shown to reduce the overall size of the power source, improve lifetime and reduce the energy loss of batteries.

Before going into details of ESs, a summary of the capacitor should be reviewed as they are similar in terms of parameters and general operating mechanisms.

1.4.5 Electrostatic Capacitor

An electrostatic capacitor consists of two conductive plates separated by a dielectric plate. The conductive plates are initially electrically neutral, and when a voltage is applied, electrons will start to travel from the positive plate to the negative plate until the potential difference between the plate is the same as the source. The two plates are now positively and negatively, and the amount of charge stored is given by Eq. 1.9, where Q is the charge stored, V is the voltage between plates, and C is the capacitance of the dielectric capacitor[41].

$$Q = CV \tag{1.9}$$

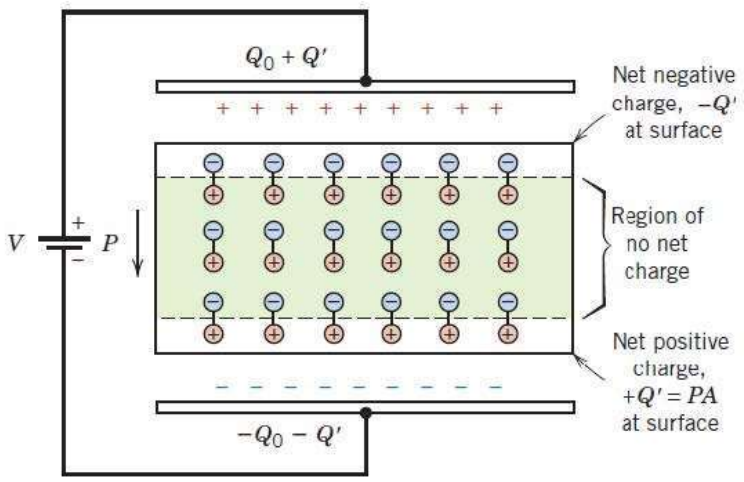

Figure 1.14: Schematic of the simple electrostatic capacitor. [41] (Figure is taken from open access internet source)

For an electrostatic capacitor, its capacitance is dependent on the dielectric constant ε_r, contact areas between plates A and the thickness of dielectric d shown in Eq. 1.10

$$C = \varepsilon_0 \varepsilon_r \frac{A}{d} \tag{1.10}$$

The equation shows that the amount of charge stored in a capacitor is proportional to voltage, and the total energy and maximum power stored in a capacitor are governed by Eq. 1.11and Eq. 1.12

$$E_{Total} = C \int_{V_{Min}}^{V_{Max}} V dV = \frac{1}{2} C V^2 \quad (1.11)$$

$$P = IV = \frac{V^2}{4R_{cap}} \quad (1.12)$$

These equations also apply to ESs, indicating the performance of capacitors can be enhanced by increasing the capacitance of electrode materials, expanding the operating voltage window, and reducing the internal resistance of capacitors.

1.4.6 Supercapacitors – Electrochemical double-layer capacitors & pseudocapacitors

A supercapacitor (SC), also called an ultracapacitor, is a high-capacity capacitor with a capacitance value much higher than other capacitors but with lower voltage limits that bridge the gap between electrolytic capacitors and rechargeable batteries. It typically stores 10 to 100 times more energy per unit volume or mass than electrolytic capacitors, can accept and deliver charge much faster than batteries, and tolerates many more charge and discharge cycles than rechargeable batteries[42]**.** Unlike ordinary capacitors, supercapacitors do not use the conventional solid dielectric, but rather, they use electrostatic double-layer capacitance and electrochemical pseudocapacitance, both of which contribute to the total capacitance of the capacitor, with a few differences.

ESs can be classified into two categories based on the charge storage mechanism[43]: (i) electrochemical double-layer capacitors (EDLCs) and (ii) pseudocapacitors.

1.4.7 Electrochemical double-layer capacitors

In EDLCs, the charge-discharge mechanism originated from pure electrostatic charge accumulation and separation at the electrode/electrolyte interface on two electrodes, as shown in Figure 1.15, and the capacitance that arises from such interface is called double-layer capacitance(Cdl) [44]. Similar to conventional capacitors, EDLCs consist of positive and

negative electrodes immersed in an electrolyte but offer a higher capacitance per volume by using high surface area porous carbon materials as active materials.

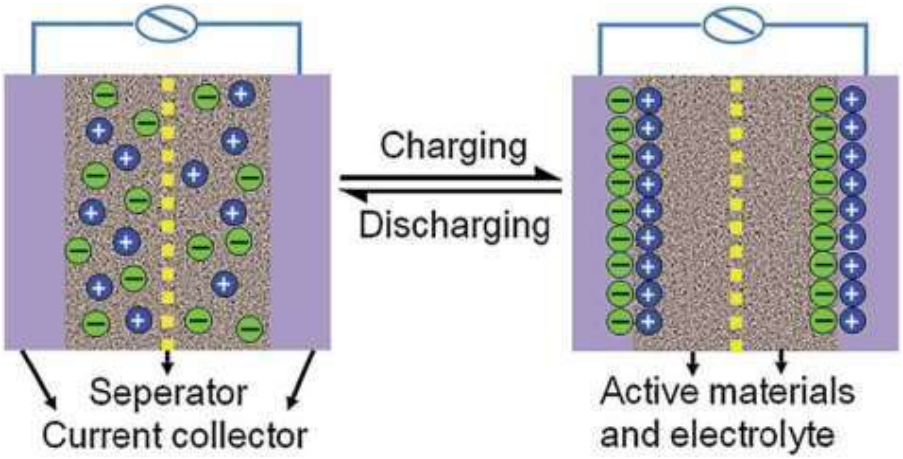

Figure 1.15: The charge storage mechanism of EDLC[45] (Figure is taken from open access internet source)

1.4.8 Principles of energy storage in EDLC

To understand the charge storage mechanism, the origin and models of double-layer should be discussed. The concept of double-layer was first modeled by von Helmholtz, and the model included two layers of opposite charges with an atomic level separation distance. Figure 1.16(a) is a schematic of the Helmholtz model, where the charged electrode surface is covered by a static array of compacted ions. After the Helmholtz model was proposed, Gouy & Chapman realized that the ions in electrolyte would not only be subjected to a static electric field on the surface of the electrode but also thermal fluctuation according to the Boltzmann principle. Therefore, Gouy-Chapman has improved the Helmholtz model by assuming ions as point charges and accounting for the thermal fluctuation shown in Figure 1.16(b). However, the assumption of point charge ions led to the failure of Gouy-Chapman model.

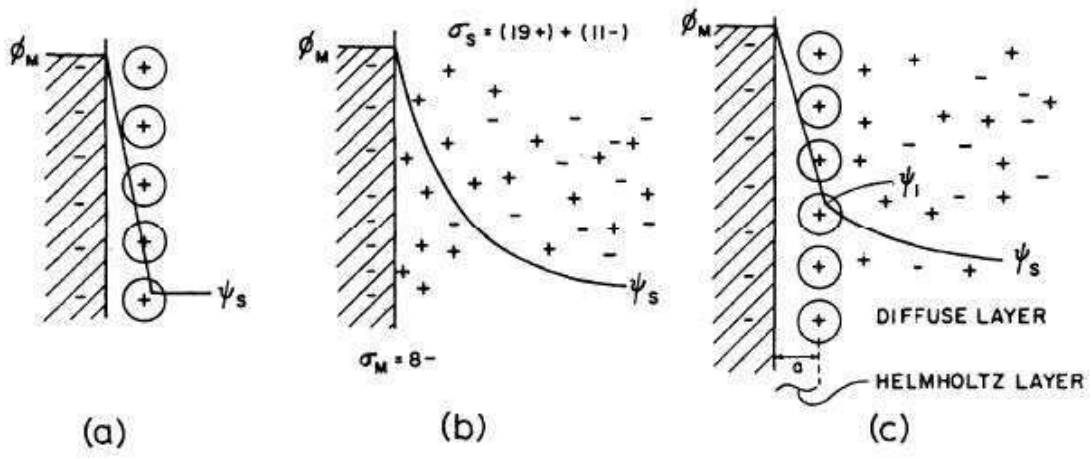

Figure 1.16: Double layer in (a) Helmholtz model, (b)Gouy-Chapman model, and (c) Stern model. [46] (Figure is taken from open access internet source)

Using the Stern model, the equivalent circuit diagram of Cdl can be represented by Figure 1.17, and the contribution of Helmholtz (C_H) and diffuse layer($C_{Diff.}$) capacitance can be related to Cdl by Eq.1.13.

Figure 1.17: Equivalent circuit diagram of Cdl in Stern model [46] (Figure is taken from open access internet source)

$$\frac{1}{C_d} = \frac{1}{C_H} + \frac{1}{C_{diff.}} \qquad (1.13)$$

Overall, the Stern model has generated a much more complete picture of the double-layer compared to Helmholtz and Gouy-Chapman model by distinguishing the contribution of capacitance from the Helmholtz layer and diffuse layer. Grahame's model further refined the Stern model, by accounting for properties of cations and anions in electrolytes such as ionic radii of ions and polarizability.[46] The most important distinction in the Grahame model is the distances of closest approach for cations and anions to the surface of the electrodes since cations are typically smaller than anions and retain a solvation shell due to ion-solvent

interaction[46]. The solvation shell of cations causes cations to be further away from the electrode surface, compared to anions. The difference in distance of closest approach for cations and anions has broken down the Helmholtz layer into inner and outer Helmholtz layers shown in Figure 1.18.

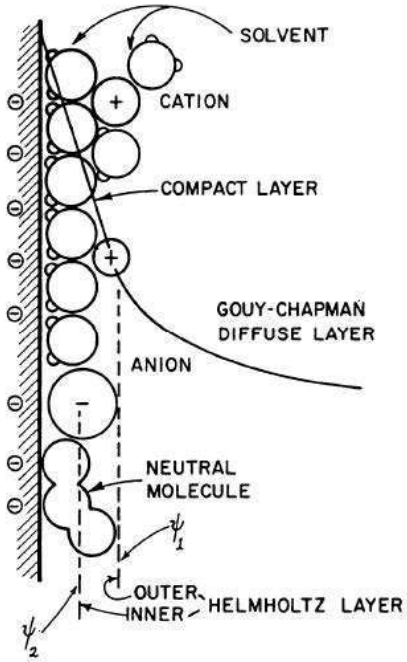

Figure 1.18: Schematic of Grahame model. [46] (Figure is taken from open access internet source)

As a result of such a difference in distance, the Cdl in positive polarization (positively charged surface) is higher than in negative polarization due to a larger separation distance. Therefore, Eq.1.13 can be rewritten as Eq.1.14, to account for the capacitance contribution from the inner (C_{IH}) and outer (C_{OH}) Helmholtz layers.

$$\frac{1}{C_{dl}} = \frac{1}{C_{IH}} + \frac{1}{C_{OH}} + \frac{1}{C_{Diff}} \qquad (1.14)$$

In commercial EDLCs, porous carbon materials are typically used as active materials, which have surface areas in the range of 500-3000 m^2 g^{-1}[47]. It has been demonstrated in the literature that these carbon-based electrodes exhibited C_{dl} between 15-50 μF cm^{-2} in aqueous

electrolytes[48]. Taking an average value of C_{dl} as 30 μF cm^{-2} and a surface area of 1000 m^2 g^{-1}, the theoretical capacitance of such carbon material is 300 F g^{-1}. However, the attainable capacitances for carbon-based materials are often below 50 F g^{-1}, due to limited electrolyte access in pores and low electrical conductivity[49]–[51]. Despite the low attainable capacitance of active materials, EDLCs operate in a pure electrostatic fashion and do not involve phase change allowing them to have an extremely long cyclic life. The operating voltage window of aqueous EDLCs is limited to about 1.4 V to prevent the decomposition of water molecules, and with organic electrolytes, EDLCs can operate up to 3.5 to 4 V[48]. Even though EDLCs with organic electrolytes give higher energy density, the electrolyte resistance is higher in organic electrolytes and reduces the power density[48].

1.4.9 Pseudocapacitors

In EDLCs, energy storage is based on charge accumulation on the surface of the electrode. In pseudocapacitors, energy is stored by fast and reversible redox reactions at the surface of active materials. Compared to EDLCs, pseudocapacitors offer 10 to 100 times higher capacitance because charge storage is not limited to the surface only, but also to the near-surface region where ions can diffuse [52]. However, the slow faradic process hindered the power performance of pseudocapacitors compared to EDLCs.

Pseudocapacitance arises when electrode potential is dependent logarithmically on the extent of reactions and involves charge transfer across the double layer[46]. Conway has identified faradic systems that can give rise to pseudocapacitance: (i) underpotential deposition system, (ii) redox pseudocapacitance, and (iii) intercalation pseudocapacitance[53].

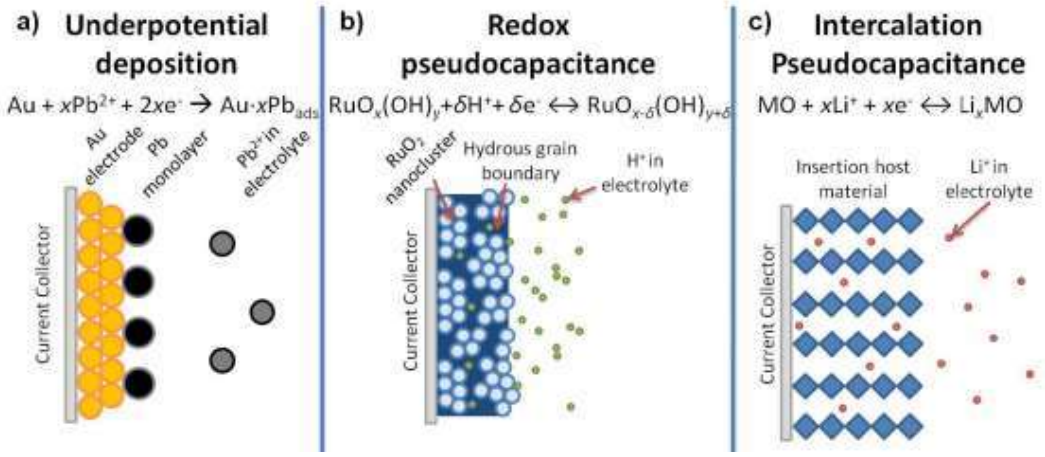

Figure 1.19: Schematic of pseudocapacitive systems identified by Conway.[53] (Figure is taken from open access internet source)

1.4.10 Principles of energy storage in pseudocapacitors

From the thermodynamic point of view, pseudocapacitance can be related to potential by Eq.1.15 where α is some property of the system, proportional to the amount of charge passed [46].

$$\frac{\alpha}{1-\alpha} = Kexp\frac{VF}{RT} \qquad (1.15)$$

In the under potential deposition system, the charge is stored by potential-dependent adsorption of adatoms (H, Pb, Cu) onto metal (Pt, Au, Ag) surface [48]. For the H-Pt system, 2-dimensional surface reactions are involved, and Eq.1.15 can be rewritten as Eq.1.16 where θ_H is the fractional surface coverage of H on Pt and CH^+ is the concentration of H^+ ions assuming the electrosorption obeys Langmuir isotherm.

$$\frac{\theta_H}{1-\theta_H} = KC_{H^+}exp\frac{VF}{RT} \qquad (1.16)$$

This equation indicated there is such a range of potential corresponds to a range of θ_H, and the capacitance can be defined by Eq.1.17.

$$C_\Phi = q_H\frac{d\theta_H}{dV} = \frac{q_H F}{RT}\theta_H(1-\theta_H) \qquad (1.17)$$

From Eq.1.17, the maximum capacitance $\frac{q_H F}{RT}$ can be reached when $\theta_H = 0.5$. Using $q_H \sim 210$ $\mu C\ cm^{-2}$, the maximum achievable capacitance for the H-Pt system is approximately 2200 $\mu F\ cm^{-2}$ [48]. However, this capacitance was derived using Langmuir isotherm with no interactions between adatoms and metals, and Boudart chemisorption typically resulted in a change in surface electron distribution[46]. Therefore, Conway and Gileadi considered an adsorption isotherm with interaction energy term $g\theta$ to accommodate for the interactions.

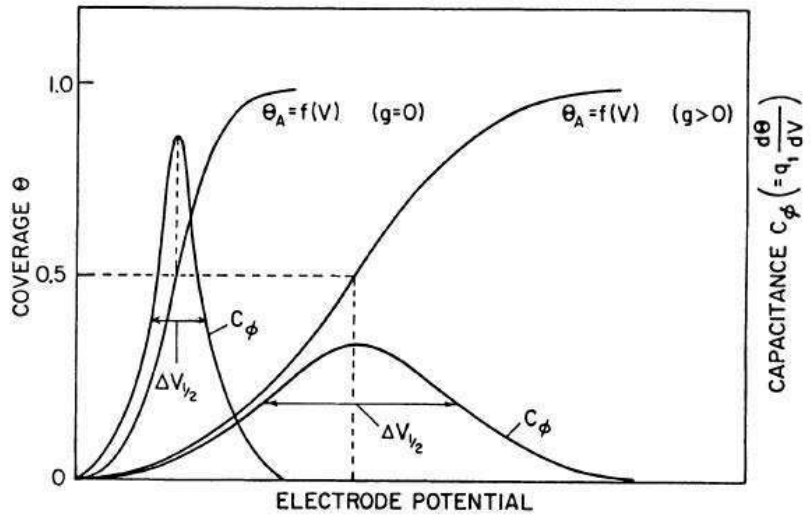

Figure 1.20: Coverage vs. the potential for positive and zero-g value. (Figure is taken from open access internet source)

To account for the interaction energy, Eq.1.17 can be modified to Eq.1.18 where maximum capacitance is achieved when $\theta_H = 0.5$, but spans over a larger potential range shown in Figure 1.20.

$$C_\Phi = \frac{q_H F}{RT} \frac{\theta(1-\theta_H)}{1+g\theta_H(1-\theta_H)} \qquad (1.18)$$

Despite the substantial pseudocapacitance arising from underpotential deposition, the high cost of noble metal substrates has limited their applications[52]. However, the concept of chemisorption and interaction energy can still be applied for redox and intercalation pseudocapacitance systems.

In redox pseudocapacitance, ions are electrochemically adsorbed onto the surface of active materials accompanied by faradic charge transfer[53]. Metal oxides and conducting polymers are examples of redox pseudocapacitive materials, and the adsorption of ions is achieved by the charge compensation in redox reactions.

For any redox reaction, it can be described using the general chemical equation of Eq.1.19, where Ox and Red are the oxidized and reduced species.

$$Ox + ze^- \leftrightarrow Red \qquad (1.19)$$

Using Eq.1.19, the Nernst equation of such a system can be written as Eq.1.20, where [Ox] and [Red] represent the concentration of oxidized and reduced species

$$E = E^\circ + \frac{RT}{zF} ln \frac{\Re}{1-\Re}, \Re = \frac{[Ox]}{[Ox]+[Red]} \qquad (1.20)$$

$$\frac{\Re}{1-\Re} = exp \frac{\Delta EzF}{RT} \qquad (1.21)$$

By manipulating the Nernst equation Eq.1.21 shows a form resembling Eq.1.15, but with the property of concern of the extent of redox reactions. Therefore, a similar conclusion can be made that the potentials follow a logarithmical relation with the extent of redox reactions. Toupin et al. have demonstrated such potential dependence in MnO_2 thin and thick film electrodes by X-ray photoelectron spectroscopy (XPS), where MnO_2 oxidation state changes with potential for thin-film electrode[54]. Another interesting finding of Toupin et al. was that the oxidation state of MnO_2 thick film did not vary with potential which they concluded the charge storage mechanism was similar to carbon electrode, and only a thin layer of MnO_2 was involved in the process and electrochemically active[54].

The intercalation pseudocapacitance is also based on redox reactions, which arise when ions intercalate into tunnels or layers of active materials accompanied by faradic charge transfer without crystallographic phase change but involve redox reactions in a 3-dimensional

structure rather than a 2-dimensional surface in redox pseudocapacitance. Similar to underpotential deposition and redox pseudocapacitance, the extent of intercalation can be related to a range of potential by Eq.1.22, where X is the fraction of ion occupancy in lattices.

$$\frac{X}{1-X} = exp\frac{\Delta EzF}{RT} \qquad (1.22)$$

Overall, Figure 2.8 shows a summary of pseudocapacitive systems and their corresponding Nernst equations, and the key idea of this section is the logarithmic relations between potential and capacitance give rise to pseudocapacitance

1.5 Electrode materials

The higher supercapacitive performance can be achieved by selecting active material with desired properties. The features of active material plays important role in achieving high supercapacitive performance. Metal oxides and hydroxides are used as active materials for pseudocapacitors, which have high theoretical capacitances originating from fast faradic reactions and resulting in a much higher energy density than EDLCs. Many metal oxides and hydroxides such as RuO_2, MnO_2, V_2O_5, NiO, Co_3O_4, Fe_2O_3, and FeOOH are some examples of materials, which have been investigated and have shown exceptional results as active materials for ESs. However, the majority of these metal oxides and hydroxides suffer from low electrical conductivity, and conductive carbon materials are incorporated to fabricate composite materials.[43], [55]

A review of electrodes developed till now is presented below

1.5.1 Ruthenium dioxide (RuO_2)

Ruthenium dioxide is one of the first metal oxides investigated for its application in ESs. Its crystalline and amorphous hydrous forms have the ideal characteristics properties of faradic active materials, such as multiple oxidation states, high electrical and ionic conductivities, and good cyclic stabilities[55]. In 1971, Trasatti et al. prepared RuO_2 thin film by thermal decomposition and the film exhibited capacitive behavior in 1M $HClO_4$ electrolyte in the

voltage range of 0 to 1.45V vs. RHE [56]. In acidic conditions, the charge storage mechanism of RuO_2 can be expressed by Eq.1.23.

$$RuO_2 + xH^+ + xe^- \leftrightarrow RuO_{2-}(OH)_x \qquad (1.23)$$

The pseudocapacitance of RuO_2 thin film was attributed to the successive redox transition from Ru^{2+} to Ru^{4+}, and the conversion of OH^- to O^{2-} within the structure by transfer of proton[55]. The performance of RuO_2 electrodes is governed by the charge transfer and diffusion processes, such as electron hopping within and between RuO_2 particles, electron transfer from active materials to current collectors, and ion diffusion within RuO_2[57]. Among the two forms of RuO_2, the hydrous form of RuO_2 has shown higher capacitance compared to the anhydrous. Sugimoto et al. have investigated the capacitive performance of RuO_2 with different water content, and they have shown anhydrous RuO_2 has a much lower capacitance (24 F g^{-1}) than the hydrous form (342 F g^{-1}) [58] and explained with the tree root model for anhydrous RuO_2, the particles are agglomerated with no available micropores for ion diffusion, and hydrous RuO_2 particles are smaller, and hydrated micropores exist between particles allowing good ion transport. Therefore, the water content in RuO_2 plays an important role, which is responsible for fast ionic conduction through the porous structure to enhance capacitive performance[58].

Despite having the ideal properties for ESs applications, the high cost of RuO_2 has limited its applications. To address this problem, some research was conducted to fabricate RuO_2 composite with low-cost metal oxides or deposition of RuO_2 on conductive substrates[59]. Hu et al. have fabricated hydrous RuO_2 – TiO_2 nanocomposite by hydrothermal process, and such electrodes have shown remarkable capacitance of 992 F g^{-1} at the scan rate of 100 mV s^{-1} [60]. In another study by Hsieh et al., composite composted of vertically aligned MWCNTs

coated with hydrous RuO_2 on a titanium current collector, and a maximum capacitance of 1652 F g^{-1} was achieved [61].

1.5.2 Manganese dioxide (MnO_2)

MnO_2 has been investigated extensively for ESs application due to its high theoretical capacitance (1370 F g^{-1}), low cost, low toxicity compared to other metal oxides, and multiple available oxidation states.[62], [59] Similar to RuO_2, the pseudocapacitance of MnO_2 is derived from the successive redox transition of Mn^{3+} and Mn^{4+}[43], and the charge storage mechanism can be expressed by Eq.1.24.

$$MnO_2 + C^+ + e^- \leftrightarrow MnOOC \qquad (1.24)$$

An advantage of MnO_2 compared to RuO_2 is its capability of operating in a mild aqueous electrolyte such as Na_2SO_4 and chloride salts (KCl, NaCl)[2], rather than strong acid or base electrolyte used in RuO_2 systems[55].

MnO_2 has various crystal structures, denoted by α, β, γ, δ, and λ phases, and is a crucial factor in the electrochemical performance of MnO_2, and all phases have tunnel structures for electrolyte access, where the tunnel size varies from 1.89 to 7 Å[63]. Brousse et al. and Devaraj et al. have determined the capacitance of different structures of MnO_2 in a 0.1M K_2SO_4 and 0.1M Na_2SO_4 solution respectively, and both authors suggested that the capacitance of MnO_2 decreases in the order of $\alpha \cong \delta > \gamma > \lambda > \beta$ [63], [64].

In another study by Ghodbane et al., the surface area of different structures of MnO_2 was investigated to determine the correlation between surface area and capacitance and showed that capacitance of MnO_2 has a strong correlation with ionic conductivities, rather than the BET surface area[65]. These results have indicated the charge storage mechanism of MnO_2 is not only limited to surface reactions but also ion intercalation into bulk MnO_2[64], [65].

Despite its high theoretical capacitance and compatibility with aqueous electrolytes, one of the major drawbacks of MnO_2 is its low electrical conductivity.[59], [62] The conductivity of electrode materials has a significant impact on the capacitance and rate performance. As the charge-discharge rate increases, the low conductivity of electrode materials limits the charge storage process in a confined volume and results in reduced capacitance and poor rate performance.

1.5.3 Vanadium pentaoxide (V_2O_5)

Other than manganese oxides, V_2O_5 has also shown remarkable performance as the active material for batteries and ESs. V_2O_5 possesses advantages such as high energy density, low toxicity, low cost, stable layered structure, and wide potential window arising from multiple available oxidation states from V^{2+} to V^{5+}[43], [53], [57], [66]. Lee and Goodenough fabricated the first amorphous $V_2O_5 \cdot nH_2O$ composite electrode by quenching V_2O_5 powder heated at 1223 K for 30 minutes in Deionised water and subsequently balled milled with acetylene black and polytetrafluoroethylene (PTFE) then pressed on a Ti substrate[67]. The fabricated electrode showed a close to mirror-image cyclic voltammogram between the potential of -0.2 to 0.8 V vs. SCE in a 2M KCl electrolyte at low pH (pH = 2.32), indicating that amorphous V_2O_5 can give pseudocapacitance in aqueous electrolyte with a specific capacitance of 346.4 F g^{-1}[67]. However, they have also found that the V_2O_5 composite electrode in 2M KCl close to the neutral electrolyte (pH = 6.67) undergoes dissolution at -0.1 V vs. SCE, and such dissolution behavior of V_2O_5 can be reduced by adjusting the pH of electrolyte to more acidic condition. Moreover, V_2O_5 also suffers from low electrical conductivity similar to MnO_2.

In an approach by Zhu et al., they have fabricated a 3D network of V_2O_5 nanosheets by producing 2D nanosheets by hydrothermal synthesis, followed by a freeze-drying procedure.

The resulted in porous 3D structure allowed high specific capacitance of 451 F g^{-1} in neutral Na_2SO_4 electrolyte, and remarkable capacitance retention of more than 90% over 4000 cycles[68]. In another approach, Qu et al. have attempted to reduce dissolution and improve conductivity using a core-shell structure of polypyrrole (PPy) on V_2O_5 nanoribbon [69]. The electrode coated with V_2O_5 of nanoribbon morphology was tested in a 0.5 M K_2SO_4 electrolyte, and the electrode has shown an exceptionally high specific capacitance of 308 F g^{-1}[69]. The electrode was also subjected to cycling for 10000 cycles, and the capacitance loss was less than 5%, whereas pure V_2O_5 resulted in a 17.5% loss[69].

1.5.4 Nickel oxide (NiO) & nickel hydroxide ($Ni(OH)_2$)

NiO is another promising candidate for ESs application, due to its extremely high theoretical capacitance of 2584 F g^{-1}, low cost, and low toxicity[70], [71]. NiO is typically synthesized by producing $Ni(OH)_2$ and subsequently annealed at high temperatures to form NiO[57]. The electrolyte for NiO electrode is usually alkaline solutions, however, the charge storage mechanism is unclear. There are two theories proposed for the pseudocapacitance of NiO arise from alkaline solutions, where the first one involves the redox reactions between NiO and nickel oxyhydroxide (NiOOH) (Eq.1.25 & 1.26), and the latter theory involves reactions between $Ni(OH)_2$ and NiOOH (Eq.1.27 & 1.28)[59]. However, it is commonly believed that Eq.1.25 occurred first to produce NiOOH, followed by the reversible redox reactions between $Ni(OH)_2$ and NiOOH[71].

$$NiO + OH^- + \leftrightarrow NiOOH + e^- \quad (1.25)$$

$$NiO + H_2O + e^- \leftrightarrow NiOOH + H^+ + e^- \quad (1.26)$$

$$N(OH)_2 \leftrightarrow NiOOH + H^+ + e^- \quad (1.27)$$

$$N(OH)_2 + OH^- \leftrightarrow NiOOH + H_2O + e^- \quad (1.28)$$

It has been shown that there are a few issues with NiO, such as significantly lower specific capacitance achievable compared to the theoretical value, low electrical conductivity, and poor cyclic stability[59]. Similar to other metal oxides, efforts have been focusing on fabricating nanostructured NiO or NiO composite with other materials[70], [72–75]. Nam et al. have investigated the electrochemical performance of porous NiO film derived from electroplated $Ni(OH)_2$ film on nickel foil substrate with different deposition current densities followed by heat treatment. The specific capacitance of NiO film increased with deposition rate, and a specific capacitance of 277 F g^{-1} was achieved in 1M KOH electrolyte for the NiO film with a deposition current density of 4 mA cm^{-2}[76]. In another investigation by Yuan et al., they fabricated porous NiO nano and microspheres to improve rate performance. The approach involved a low-temperature precipitation reaction with an alkaline solution and nickel salts, and the fabricated electrode exhibited a specific capacitance of 525F g^{-1} at the current density of 4 A g^{-1}[77]. The hierarchical porosity generated by the nano and microspheres has offered high capacitance retention of 98% after 2000 cycles[77].

$Ni(OH)_2$ has a hexagonal layered structure with two polymorphs, α-$Ni(OH)_2$ and β-$Ni(OH)_2$, and have been demonstrated that the structure has an impact on the performance of the electrodes[78]. α-$Ni(OH)_2$ has intercalated with anions and water within the structure, whereas water is absent in β-$Ni(OH)_2$[78]. The α-$Ni(OH)_2$ showed a higher specific capacitance than β-$Ni(OH)_2$, and the situation can be explained by recalling that hydrous RuO_2 showed higher specific capacitance than the anhydrous form due to improved ion transport[58], [79], [80].

1.5.5 Cobalt oxide (Co_3O_4) & cobalt hydroxide ($Co(OH)_2$)

Co_3O_4 is another alternative active material for ESs application, given a high theoretical capacitance of 3560 F g^{-1}, low cost, good corrosion resistance, and high electrochemical stability[43], [71]. Co_3O_4 electrodes can be operated in alkaline solutions, and the charge storage mechanism is described in Eq.1.29.

$$Co_3O_4 + H_2O + OH^- \leftrightarrow 3CoOOH + e^- \qquad (1.29)$$

Despite its high theoretical capacitance, the actual capacitance achievable by Co_3O_4 is low, and the poor conductivity is one of the major challenges[81]. Nanostructured Co_3O_4 has been fabricated such as nanotubes[81], nanosheets[82], nanotubes[83], nanowire arrays[84], and composite with graphene[85] and porous carbon[83] were also investigated. Salunkle et al. have to synthesize nanoporous Co_3O_4 using a metal-organic framework. The nanoporous structure has allowed a large surface area for charge storage, and the electrode exhibited a specific capacitance of 504 F g^{-1} at a scan rate of 5 mV s^{-1} in a 6M KOH electrolyte[83].The cyclic stability of the electrode was also tested, and interestingly the specific capacitance increased to ~1100 F g^{-1} after 500 cycles and plateau afterward [84]. The authors suggested that the phenomenon was a result of an activation process, where the electrode allowed more complete intercalation and deintercalation during charge-discharge.

$Co(OH)_2$ has also gained significant interest due to its layered structure with large spacings, and it can facilitate fast ions motions during intercalation and deintercalation[59]. However, to retain the structure of hydroxide, the potential window of $Co(OH)_2$ is limited to around 0.5 V[85], [86]. Kong et al. have synthesized asymmetric supercapacitor with α-$Co(OH_)_2$ and AC, and the α-$Co(OH)_2$ electrode has shown remarkable specific capacitance of 735 F g^{-1} in the potential range of 0 to 0.4 V vs. SCE, and the device fabricated has a specific capacitance of 72.4 F g^{-1} within the potential window of 0-1.6 V[86]. Jagadale et al. have investigated the

electrochemical performance of β-$Co(OH)_2$ thin film deposited on stainless steel substrate potentio-dynamically, the electrode exhibited outstanding specific capacitance of 890 F g^{-1} in 1M KOH electrolyte in the potential window of -0.2 to 0.4 V vs. SCE[87].

1.5.6 Transition metal oxalate-based electrodes

Other than transition metal oxide, oxalate-based metal-organic framework (MOF) has also shown performance as an active material for ESs. MOF possesses advantages such as high energy density, low toxicity, low cost, stable pores structure, and wide potential window arising from multiple available oxidation states[88]. and the charge storage mechanism is described by Eq.1.30.

$$M(II)C_2O_4.\ nH2O + OH^-_{solu} \longleftrightarrow M(III) - (OH^-)C_2O_4.nH_2O + e^- \quad (1.30)$$

Wang et al. have to synthesize $Ni_{0.55}Co_{0.45}C_2O_4$ solid solution by the liquid-liquid interfacial reaction involving a co-precipitation process and get a micro-cuboid structure composed of nanoparticles with sizes ranging from 13 to 23 nm. Moreover, electrochemical measurements achieved a specific capacity of 562 C g^{-1} at a current density of 1 Ag^{-1}[89]. In another investigation, Zhao et. al. demonstrated the use of (Ni–OA) for ESs application. They prepared the electrode 2D porous Ni-OA thin sheets by the direct hydrothermal decomposition of a mixed aqueous solution of transition metal nitrates ($Ni(NO_3)_2$ and OA. The fabricated electrode was tested in a 6 M KOH electrolyte and showed a specific capacitance of 2835.06 F.g^{-1} at 1.0 Ag^{-1}. The cyclic stability of the electrode was also tested (94.3 % of capacity retention after 5,000 cycles at 10 A·g^{-1}) [90]. Pu et. al. have synthesized 2D porous Co-OA thin sheets with different sizes and crystallinity assembled by interconnected nanosheet frameworks by hydrothermal strategy at 220 °C for different reaction times. The electrode was tested in a 6 M KOH electrolyte and showed specific capacitance(1.631 F·cm^{-2} at the current density of 1.2 mA·cm^{-2}. the retention rate was 80.6 %

when the current density increased 10 times [91]. Cheng et. al. have synthesized nanostructured cobalt oxalate electrodes by one-step in-situ electrochemical method (anodization). The prepared electrode was demonstrated in KOH electrolyte and showed a specific capacitance of 1269 F g^{-1} at the current density of 6 A g^{-1} in the galvanostatic charge/discharge test. Moreover, the electrode also tested rate capability and cycling stability (8.1% decay after 100,000 cycles)[92],

1.5.7 Intercalation pseudocapacitance in Nb_2O_5

Intercalation pseudocapacitance is a charge storage phenomenon characterized by ion insertion into a layered or tunnel structure. Even though such a mechanism results in a change of potential with the amount of ion insertion, it is not considered capacitive due to the kinetic limitations of solid-state diffusion. This limitation renders most intercalation-based materials suitable for timescales where charge storage occurs in hours, as in batteries. In other studies, the exceptionally rapid charge storage of Nb_2O_5 nanocrystals was demonstrated in a non-aqueous Li^+ electrolyte and it was shown that the charge storage was capacitive, later the kinetics of charge storage in Nb_2O_5 are quantified and, in the process, several characteristics necessary for intercalation pseudocapacitance were defined: a crystalline structure that offered 2D transport pathways and little structural change upon intercalation, currents that vary inversely with time, charge storage capacity that is mostly independent of rate, and redox peaks that exhibit small voltage offsets, even at high rates. The principal benefit realized from intercalation pseudocapacitance is that high levels of charge storage are achieved within short periods because there are no limitations from solid-state diffusion.

The phenomenon of intercalation pseudocapacitance and the high-rate behavior of Nb_2O_5 were investigated by using two different electrode techniques that provide a wide variation in sweep rates. For timescales between ~3 hours and 60 seconds (sweep rates of 0.1-20 mV s^{-1}

within a voltage window of 1.2 V), a thin-film electrode was utilized. For shorter timescales where ohmic polarization is significant (60-500 mV s^{-1}), a cavity microelectrode was used where the active material was mixed with conductive carbon black to alleviate the loss of electrical transport (ohmic losses) [93].

The results presented in the study Nb_2O_5 exhibit electrochemical features of a pseudocapacitive material despite charge storage occurring in the bulk. Such behavior is consistent with intercalation pseudocapacitance. The electrochemical features indicated in this mechanism are currents that are linearly proportional to the sweep rate, the capacity that does not vary significantly with charging time, and peak potentials that do not shift significantly with the sweep rate. A key "design rule" for intercalation pseudocapacitance at the atomic scale is a structure that does not undergo phase transformations upon intercalation. In addition, facile 2D lithium-ion diffusion pathways are important. Charge storage that behaves as a quasi-2D process exhibits similar behavior to 2D surface adsorption reactions[52]. These features contrast with those of pseudocapacitive $RuO_2 \cdot xH_2O$ where charge storage occurs mainly on the surface or near-surface [53][94-95].

In this thesis, I focused on the development of novel materials to be intercalative pseudocapacitive electrodes. Metal oxalate framework structures are employed here to develop superior electrodes for hybrid intercalative battery-type supercapacitors. Thermochemical properties especially coupling of TGA/DTA techniques with strategic precipitation schemes to develop novel highly porous nanostructures that can enable fast transport or diffusion of ions in the host structure to have large-scale charge storage capabilities is the main focus of the thesis. Further, the focus of the thesis is to understand the diffusion kinetics of the electrode to develop superior battery-type redox-mediated intercalative supercapacitors.

References:

1. K. Handayani, Y. Krozer, T. Filatova, From fossil fuels to renewables: an analysis of long-term scenarios considering technological learning Energy Pol,2019, 127,134-146,.
2. Global Energy Review 2019. Glob. Energy Rev. 2019 ,2020
3. United nation climate action https://www.un.org/en/climatechange/what-is-renewable-energy
4. Esd solar energy https://esdsolar.com/how-does-solar-energy-work/
5. Wind energy https://energy.economictimes.indiatimes.com/
6. Geothermal energy https://en.wikipedia.org/wiki/Geothermal_energy
7. Hydrothermal energy https://www.swapdial.com/
8. The International Renewable Energy Agency (IRENA), Ocean energy https://www.irena.org/ocean
9. Bioenergy basics https://www.energy.gov/eere/bioenergy/bioenergy-basics
10. Kazuya Kubo, Yoshinori Kawaharazaki, Hideaki Itoh. Development of large MH tank system for renewable energy storage. International journal of hydrogen energy; 2017, 4, 22475 – 22479.
11. Pascal Dubucq, Prof.Dr.-Ing.Guunter Ackermann. Optimal Use of Energy Storage Potentials in a Renewable Energy System with District Heating. Energy Procedia; 2017, 135:158 -171.
12. Mustafa E. Amiryar and Keith R. Pullen. A Review of Flywheel Energy Storage System Technologies and Their Applications. Applied Sciences 2017.
13. Electrical Funda Blog. Flywheel as Energy Storage Device, Calculations and Rotor Requirements.http://electricalfundablog.com/flywheel-energy-storage-calculations-rotor.

14. Xing Luo, Jihong Wang, Mark Dooner, Jonathan Clarke. Overview of current development in electrical energy storage technologies and the application potential in power system operation. Applied Energy; 2015, 137: 511–536.
15. Diaz-Gonzalez F, Sumper A, Gomis-Bellmunt O, Villafafila,Robles R. A review of energy storage technologies for wind power applications. Renewable Sustanable Energy; 2012,16:2154–71.
16. Hydrogen Energy Storage: A New Solution To the Renewable Energy Intermittency Problem. http://www.renewableenergyworld.com/articles/2014/07/hydrogen-energy-storage-a-new-solution-to-the-renewable-energy-intermittency-problem.html
17. Amit Kumar Rohit, Ksh. Priyalakshmi Devi, Saroj Rangnekar. An overview of energy storage and its importance in Indian renewable energy sector. Journal of Energy Storage; 2017, 13:10–23.
18. Buckles, W. & Hassenzahl, W., 2000. Superconducting Magnetic Energy Storage. IEEE Power Engineering review; 2020, 16: 16–20.
19. Energy Storage Sense. Superconducting Magnetic Energy Storage. http://energystoragesense.com/superconducting-magnetic-energy-storage-smes/
20. IEA-ETSAP and IRENA. Thermal Energy Storage Technology Brief E17, 2013
21. Satyawan Singh, Pradeep Kumar Sharma, Neeru Goyal, Prashant KumarTayal. Thermal Energy Storage: A Process To Increase Efficiency and To Save our Environment. ICLISEM; 2016, 81-87.
22. Joseph Stekli, Levi Irwin and Ranga Pitchumani. Technical Challenges and Opportunities for Concentrating Solar Power With Thermal Energy Storage. Journal of Thermal Science and Engineering Applications ., 2013, 5(2).
23. H. Ibrahim, A. Ilinca, J. Perron, Energy Storage Systems-Characteristics and Comparisons, Renewable and Sustainable Energy Reviews, 2008, 12, 1221.

24. M. M. Titirici, R. J. White, C. Falco, M. Secilla, Black Perspectives for a Green Future: Hydrothermal Carbons for Environment Protection and Energy Storage, Energy and Environ. Sci.,2012, 5, 6796.
25. James, F. A. J. L. Michael Faraday's First Law of Electrochemistry: How Context Develops New Knowledge. Electrochemistry: Past and Present 1983, 32–47.
26. History of the battery, https://en.wikipedia.org/wiki/History_of_the_battery
27. Das Gupta, S. The Search for Portable Electricity: History of High Energy-Density Batteries. Electrochemistry: Past and Present, 1989, 543–553.
28. Becker, H. E. Low voltage electrolytic capacitor. U.S. Patent #2800616 (1957).
29. Huggins, R. A. Advanced Batteries: Materials Science Aspects.,Springer: New York, 2009.
30. Petr Krivik, Petr Baca. "Electrochemical Energy Storage". Energy Storage-Technologies and Applications , IntechOpen,2013 ,80-100;. doi:10.5772/52222:.
31. Pavlov, Detchko. Lead-acid batteries: science and technology. Elsevier, 2011.
32. M.Calabek, K.Micka, P.Baca, A fundamental study of the effects of compression on the performance of lead accumulator plates,. Journal of Power Sources, 2001 95, 97-107.
33. J. B.,Goodenough & Park, K.-S. The Li-ion rechargeable battery: a perspective. Journal of the American Chemical Society, 2013, 135, 1167–1176.
34. J.-M., Tarascon & Armand, M. Issues and challenges facing rechargeable lithium batteries. Nature 2001, 414, 359–367.
35. C. A. Vincent, & Scrosati, B. Modern Batteries: An Introduction to Electrochemical Power Sources.Butterworth-Heinemann: Oxford, 1997.
36. Jeong, H.S., Hong, S.C., Lee, S.Y., Effect of microporous structure on thermal shrinkage and electrochemical performance of Al2O3/poly(vinylidene fluoride-

hexafluoropropylene) composite separators for lithium-ion batteries. J. Membr. Sci.,2010, 364, 177–182.

37. Cong-Ling, H., Jie, W., Miao, Z., Jin-Ming, Y., Jin-Peng, L., Application of adaptive algorithm of solar cell battery charger,Proceedings of the 2004 IEEE international conference on electric utility deregulation, restructuring and power technologies, 2004, 2, 810–813.
38. Zheng, H., Cathode performance as a function of inactive material and void fractions. J. Electrochem. Soc.,2010, 157, A1060–A1066.
39. Christensen, J. et al., A critical review of Li/air batteries. J. Electrochem. Soc.,2012, 159, R1–R30.
40. Tang, Y. et al., Experimental investigation of dynamic performance and transient responses of a kW-class PEM fuel cell stack under various load changes. Appl. Energy, 2010, 87, 1410–1417.
41. W. D. Callister, Materials Science and Engineering: An Introduction, 8th ed. John Wiley & Sons Inc.
42. Häggström F, Delsing J. IoT Energy Storage - A Forecast. Energy Harvesting and Systems.; 2018, 5(3-4): 43-51.
43. G. Wang, L. Zhang, and J. Zhang, "A review of electrode materials for electrochemical supercapacitors," Chem Soc Rev, 2012, 41, 797–828.
44. P. Sharma and T. S. Bhatti, "A review on electrochemical double-layer capacitors," Energy Convers. Manag., 2010, 51,2901–2912.
45. T. Chen and L. M. Dai , Carbon nanomaterials for high-performance supercapacitors Mater. Today.,2013, 16 , 272-280.
46. B. E. Conway, Electrochemical Supercapacitors: Scientific Fundamentals and Technological Applications. Boston, MA: Springer US, 1999.

47. H. Zhang, W. Zhang, J. Cheng, G. Cao, and Y. Yang, “Acetylene black agglomeration in activated carbon based electrochemical double layer capacitor electrodes,” Solid State Ion.,2008, 179,1946–1950.

48. B. E. Conway, V. Birss, and J. Wojtowicz, “The role and utilization of pseudocapacitance for energy storage by supercapacitors,” J. Power Sources, 1997, 66, no. 1–2, 1–14.

49. H. Nakagawa, A. Shudo, and K. Miura, “High-Capacity Electric Double-Layer Capacitor with High-Density-Activated Carbon Fiber Electrodes,” J. Electrochem. Soc., 2000, 147,38.

50. H. Tamai, M. Kunihiro, M. Morita, and H. Yasuda, “Mesoporous activated carbon as electrode for electric double layer capacitor,” J. Mater. Sci.,2005, 40, 3703–3707.

51. V. V. N. Obreja, “On the performance of supercapacitors with electrodes based on carbon nanotubes and carbon activated material—A review,” Phys. E Low-Dimens. Syst. Nanostructures, 2008, 40, 2596–2605.

52. B. E. Conway, “Transition from ‘Supercapacitor to Battery’ Behavior in Electrochemical Energy Storage,”J. Electrochem. Soc.,1991, 138 ,1539-1544.

53. V. Augustyn, P. Simon, and B. Dunn, “Pseudocapacitive oxide materials for high-rate electrochemical energy storage,” Energy Environ. Sci.,2014, 7, 1597-1601.

54. M. Toupin, T. Brousse, and D. Bélanger, “Charge Storage Mechanism of MnO_2 Electrode Used in Aqueous Electrochemical Capacitor,” Chem. Mater.,2004,16, 3184–3190.

55. M. Y. Ho, P. S. Khiew, D. Isa, T. K. Tan, W. S. Chiu, and C. H. Chia, “A review of metal oxide composite electrode materials for electrochemical capacitors,” Nano, 2014, 09, 143-149.

56. Trasatti, S. & Buzzanca, G. Ruthenium dioxide: a new interesting electrode material. Solid state structure and electrochemical behaviour. Electroanalytical chemistry and interfacial electrochemistry, 1971, 29, 1–5.

57. C. D. Lokhande, D. P. Dubal, and O.-S. Joo, "Metal oxide thin film based supercapacitors," Curr. Appl. Phys.,2011, 11, 255–270.

58. W. Sugimoto, H. Iwata, K. Yokoshima, Y. Murakami, and Y. Takasu, "Proton and Electron Conductivity in Hydrous Ruthenium Oxides Evaluated by Electrochemical Impedance Spectroscopy: The Origin of Large Capacitance," J. Phys. Chem. B,2005, 109, 7330–7338.

59. F. Shi, L. Li, X. Wang, C. Gu, and J. Tu, "Metal oxide/hydroxide-based materials for supercapacitors," RSC Adv, 2014, 4, 41910–41921.

60. C.-C. Hu, Y.-L. Yang, and T.-C. Lee, "Microwave-Assisted Hydrothermal Synthesis of RuO[sub 2]·xH[sub 2]O–TiO[sub 2] Nanocomposites for High Power Supercapacitors," Electrochem. Solid-State Lett.,2010, 13, 173-185.

61. T.-F. Hsieh, C.-C. Chuang, W.-J. Chen, J.-H. Huang, W.-T. Chen, and C.-M. Shu, "Hydrous ruthenium dioxide/multi-walled carbon-nanotube/titanium electrodes for supercapacitors," Carbon, 2012, 50,1740–1747.

62. M. Huang, F. Li, F. Dong, Y. X. Zhang, and L. L. Zhang, "MnO_2 -based nanostructures for high-performance supercapacitors," J. Mater. Chem. A,2015, 3, 21380–21423.

63. S. Devaraj and N. Munichandraiah, "Effect of Crystallographic Structure of MnO_2 on Its Electrochemical Capacitance Properties," J. Phys. Chem. C,2008, 112, 4406–4417.

64. T. Brousse, M. Toupin, R. Dugas, L. Athouël, O. Crosnier, and D. Bélanger, "Crystalline MnO[sub 2] as Possible Alternatives to Amorphous Compounds in

Electrochemical Supercapacitors," J. Electrochem. Soc.,2006 vol. 153, no. 12, p. A2171.

65. O. Ghodbane, J.-L. Pascal, and F. Favier, "Microstructural Effects on Charge-Storage Properties in MnO_2 -Based Electrochemical Supercapacitors," ACS Appl. Mater. Interfaces,2009, 1, 1130–1139.
66. B. Saravanakumar, K. K. Purushothaman, and G. Muralidharan,"Interconnected V_2O_5 Nanoporous Network for High-Performance Supercapacitors," ACS Appl. Mater. Interfaces,2012, 4,4484–4490.
67. H. Y. Lee and J. B. Goodenough, "Ideal Supercapacitor Behavior of Amorphous $V_2O_5{\cdot}nH_2O$ in Potassium Chloride (KCl) Aqueous Solution," J. Solid State Chem., 1999, 148,81–84.
68. J. Zhu ., "Building 3D Structures of Vanadium Pentoxide Nanosheets and Application as Electrodes in Supercapacitors," Nano Lett.,2013, 13, 5408–5413.
69. Q. Qu, Y. Zhu, X. Gao, and Y. Wu, "Core-Shell Structure of Polypyrrole Grown on V_2O_5 Nanoribbon as High Performance Anode Material for Supercapacitors," Adv. Energy Mater.,2012, 2,950–955.
70. J. W. Lee, T. Ahn, J. H. Kim, J. M. Ko, and J.-D. Kim, "Nanosheets based mesoporous NiO microspherical structures via facile and template-free method for high performance supercapacitors," Electrochimica Acta, 2011, 56, 4849–4857.
71. Y. Wang, J. Guo, T. Wang, J. Shao, D. Wang, and Y.-W. Yang, "Mesoporous Transition Metal Oxides for Supercapacitors," Nanomaterials, 2015,5,1667–1689.
72. S.-I. Kim, J.-S. Lee, H.-J. Ahn, H.-K. Song, and J.-H. Jang, "Facile Route to an Efficient NiO Supercapacitor with a Three-Dimensional Nanonetwork Morphology," ACS Appl. Mater. Interfaces,2013, 5,1596–1603.

73. C.-Y. Cao, W. Guo, Z.-M. Cui, W.-G. Song, and W. Cai, "Microwave-assisted gas/liquid interfacial synthesis of flowerlike NiO hollow nanosphere precursors and their application as supercapacitor electrodes," J. Mater. Chem.,2011, 21,3204-3213.
74. K.-C. Liu and M. A. Anderson, "Porous Nickel Oxide/Nickel Films for Electrochemical Capacitors," J Electrochem Soc, 1996, 143,7-9.
75. X. Zhang., "Synthesis of porous NiO nanocrystals with controllable surface area and their application as supercapacitor electrodes," Nano Res.,2010, 3 643–652.
76. K.-W. Nam and K.-B. Kim, "A Study of the Preparation of NiO[sub x] Electrode via Electrochemical Route for Supercapacitor Applications and Their Charge Storage Mechanism," J. Electrochem. Soc., 2002,149,346-349.
77. C. Yuan, X. Zhang, L. Su, B. Gao, and L. Shen, "Facile synthesis and self-assembly of hierarchical porous NiO nano/micro spherical superstructures for high performance supercapacitors," J. Mater. Chem.,2009, 19,5772-5804.
78. Y. Ren and L. Gao, "From Three-Dimensional Flower-Like α-$Ni(OH)_2$ Nanostructures to Hierarchical Porous NiO Nanoflowers: Microwave-Assisted Fabrication and Supercapacitor Properties: Rapid Communications of the American Ceramic Society," J. Am. Ceram. Soc.,2010, 93, 3560–3564.
79. H. Du, L. Jiao, K. Cao, Y. Wang, and H. Yuan, "Polyol-Mediated Synthesis of Mesoporous α-$Ni(OH)_2$ with Enhanced Supercapacitance," ACS Appl. Mater. Interfaces; 2013, 5,6643–6648.
80. M. C. Bernard, P. Bernard, M. Keddam, S. Senyarich, and H. Takenouti, "Characterisation of new nickel hydroxides during the transformation of α $Ni(OH)_2$ to β $Ni(OH)_2$ by ageing," Electrochimica Acta; 1996, 41,91–93.

81. J. Xu, L. Gao, J. Cao, W. Wang, and Z. Chen, "Preparation and electrochemical capacitance of cobalt oxide (Co_3O_4) nanotubes as supercapacitor material," Electrochimica Acta; 2010, 56, 732–736.

82. S. Xiong, C. Yuan, X. Zhang, B. Xi, and Y. Qian, "Controllable Synthesis of Mesoporous Co_3O_4 Nanostructures with Tunable Morphology for Application in Supercapacitors," Chem. - Eur. J., 2009, 15,5320–5326.

83. R. R. Salunkhe, J. Tang, Y. Kamachi, T. Nakato, J. H. Kim, and Y. Yamauchi, "Asymmetric Supercapacitors Using 3D Nanoporous Carbon and Cobalt Oxide Electrodes Synthesized from a Single Metal–Organic Framework," ACS Nano;2015, 9,6288–6296.

84. X.-C. Dong., "3D Graphene–Cobalt Oxide Electrode for High-Performance Supercapacitor and Enzymeless Glucose Detection," ACS Nano, 2012, 6, 3206–3213.

85. T. Zhao, H. Jiang, and J. Ma, "Surfactant-assisted electrochemical deposition of α-cobalt hydroxide for supercapacitors," J. Power Sources,2011, 196, 860–864.

86. L.-B. Kong, M. Liu, J.-W. Lang, Y.-C. Luo, and L. Kang, "Asymmetric Supercapacitor Based on Loose-Packed Cobalt Hydroxide Nanoflake Materials and Activated Carbon," J. Electrochem. Soc.; 2009, 156, 1000-1012.

87. A. D. Jagadale, V. S. Jamadade, S. N. Pusawale, and C. D. Lokhande, "Effect of scan rate on the morphology of potentiodynamically deposited β-$Co(OH)_2$ and corresponding supercapacitive performance," Electrochimica Acta; 2012, 78,92–97.

88. D. P. Dubal, O. Ayyad, V. Ruiz and P. Gomez-Romero, "Hybrid energy storage: the merging of battery and supercapacitor chemistries" Chem. Soc. Rev., 2015, 44, 1777–1790.

89. Wang, L.; Zhang, R.; Jiang, Y.; Tian, H.; Tan, Y.; Zhu, K.; Yu, Z.; Li, W. Interfacial synthesis of micro-cuboid $Ni_{0.55}Co_{0.45}C_2O_4$ solid solution with enhanced

electrochemical performance for hybrid supercapacitors. Nanoscale,2019, 11, 13894−13902.

90. Zhao, C.; Jiang, Y.; Liang, S.; Gao, F.; Xie, L.; Chen, L. Twodimensional porous nickel oxalate thin sheets constructed by ultrathin nanosheets as electrode materials for high-performance aqueous supercapacitors. CrystEngComm., 2020, 22, 2953.
91. Pu, T.; Li, J.; Jiang, Y.; Huang, B.; Wang, W.; Zhao, C.; Xie, L.; Chen, L. Size and crystallinity control of two-dimensional porous cobalt oxalate thin sheets: tuning surface structure with enhanced performance for aqueous asymmetric supercapacitors. Dalton Trans.,2018, 47, 9241.
92. Cheng, G.; Si, C.; Zhang, J.; Wang, Y.; Yang, W.; Dong, C.; Zhang, Z. Facile fabrication of cobalt oxalate nanostructures with superior specific capacitance and super-long cycling stability. J. Power Sources.,2016, 312, 184−191.
93. Come, J., Taberna, P.-L., Hamelet, S., Masquelier, C. & Simon, P. Electrochemical Kinetic Study of $LiFePO_4$ Using Cavity Microelectrode. Journal of The Electrochemical Society 2011, 158,1090–093.
94. Dmowski, W., Egami, T., Swider-Lyons, K. E., Love, C. T. & Rolison, D. R. Local Atomic Structure and Conduction Mechanism of Nanocrystalline Hydrous RuO_2 from X-ray Scattering. The Journal of Physical Chemistry B.,2002, 106, 12677–12683.
95. 74. Liu, Y., Zhou, F. & Ozolins, V. Ab Initio Study of the Charge-Storage Mechanisms in RuO_2 -Based Electrochemical Ultracapacitors. Journal of Physical Chemistry C., 2012, 116, 1450–1457.